Journal of Fluorescence (2019) 29:577–586
https://doi.org/10.1007/s10895-019-02374-4

ORIGINAL ARTICLE

A Highly Selective Fluorescence "Turn on" and Absorbance-Ratiometric Detection of Al^{3+} in Totally H_2O and its Application in Test Paper

Xue-Jiao Sun[1] · Yu-Qing Ma[1] · Hong Fu[1] · Zhi-Yong Xing[1] · Zhi-Gang Sun[1] · Yue Shen[1] · Jin-Long Li[2]

Received: 17 February 2019 / Accepted: 25 March 2019 / Published online: 2 April 2019

Abstract

A novel naphthalene based fluorescence probe **NBDH** was designed and synthesized. Probe **NBDH** exhibited highly selective and sensitive responses towards Al^{3+} in HEPES-NaOH buffer solution (pH = 7.4). In addition, the detection of **NBDH** to Al^{3+} could be achieved through dual channels embodied in significant fluorescent turn-on signal and ratiometric absorbance response. The stoichiometry ratio of **NBDH**-Al^{3+} was 1:1 by fluorescence job' plot and binging mechanism was further varified by the FT-IR, NMR titration and HRMS. Furthermore, **NBDH** was achieved in real sample detection, and a series of color test paper were developed for visual detecting Al^{3+} ions.

Keywords Fluorescence · Naphthalene · Al^{3+} · Test paper · Ratiometric absorbance

Introduction

Aluminum, the third most abundant metallic element in the earth, is widely used in industrial production, aeronautical material and food additives. Moreover, Al^{3+} ions, the most common ionic style of aluminum, widespread exist in water environment and tissues in the body of animals and plants [1–5]. However, lots of diseases [6–10], such as Alzheimer's disease and Parkinson's disease, amyotrophic sclerosis, microcytic hypochromic anemia, encephalopathy, dementia and myopathy, may be derived from the excess level of Al^{3+} in human body. So, it is urgent to put indispensable efforts to develop efficient and convenient approach to detect Al^{3+} ions.

Fluorescence sensing of specific ions with suitable probes has attracted keen interest of worldwide researchers because of its high selectivity, low cost and easy performances [11–15]. However, the development fluorescence probes for Al^{3+} are much more difficult than for other metal ions duo to the shortcomings of Al^{3+} in weak ability in coordination, easier formation of $Al(OH)_3$ in water, and deficiency in spectroscopic characteristics [16–18]. Moreover, many Al^{3+} fluorescence probes have been developed with various fluorophores through different response mechanisms [19–35], but a lot of them have their limitations either in water solubility or disturbing by other metal ions, especially the Cu^{2+} which is a fluorescent quencher widely reported by many articles. All of these defects further restricted their application of Al^{3+} detection in environment and in vivo. Therefore, it is necessarily importance to develop highly selectivity and water soluble fluorescence probes.

Naphthalene fluorophore has been extensively used for the exploiting fluorescence probes because of its high stability and quite good water solubility and easy to modification [36–45]. In addition, schiff base ligand, including the unit (–C=N–), usually acted as an excellent chelating site in sensing different metal ions, therefore leading to significant change in optical signal [46–59]. Taking above statements into consideration, we designed an easy-prepared schiff-based probe **NBDH** using the naphthalene as the signaling unit. Probe **NBDH** showed distinguished fluorescent turn-on (400-fold)

Electronic supplementary material The online version of this article (https://doi.org/10.1007/s10895-019-02374-4) contains supplementary material, which is available to authorized users.

✉ Zhi-Yong Xing
zyxing@neau.edu.cn

✉ Jin-Long Li
jinlong141@163.com

[1] Department of Applied Chemistry, College of Science, Northeast Agricultural University, Harbin 150030, People's Republic of China

[2] School of Chemistry and Chemical Engineering, Qiqihar University, Qiqihar 161006, People's Republic of China

to Al^{3+} and highly selectivity without interference of other metal ions including the Cu^{2+} in totally water solution (pH = 7.4). The interaction mechanism between **NBDH** and Al^{3+} was investigated by the various spectroscopic techniques including FT-IR, ^{1}H NMR titration and HRMS. Furthermore, chemosensor **NBDH** was achieved in detection of Al^{3+} in real water samples, and a colorimetric method on filter paper for estimating the existence of Al^{3+} was also investigated.

Experimental

Materials and Reagents

All chemicals and reagents were obtained from commercial sources and used as received. ^{1}H NMR and ^{13}C NMR spectra were recorded on a Bruck AV-600 spectrometer using TMS as the internal standard, and chemical shifts were showed in ppm. Mass spectra were measured using a Waters Xevo UPLC/G2-SQ Tof MS spectrometer. The FT-IR spectrum was recorded on a Perkin-Elmer IR spectrophotometer using KBr pellet. Melting point was measured with Beijing Taike melting point apparatus. Fluorescence spectra were measured on a Perkin Elmer LS55 fluorescence spectrometer. Absorption spectra were recorded using a Pgeneral TU-2550 UV-vis spectrophotometer.

Stock solution of the **NBDH** (1×10^{-5} M) and all metal ions (1×10^{-2} M) (Na^+, K^+, Ca^{2+}, Mg^{2+}, Ba^{2+}, Cr^{3+}, Mn^{2+}, Fe^{2+}, Fe^{3+}, Cu^{2+}, Ag^+, Co^{2+}, Ni^{2+}, Zn^{2+}, Cd^{2+}, Al^{3+} and Pb^{2+}) were prepared in H_2O medium. These resulting solutions were maintained at room temperature for 5 min, and then the spectral properties were measured. The spectral detected at different pH which was adjusted by using 0.1 M NaOH and 0.1 M HEPES. Both the excitation and emission slits were set at 10 nm. The fluorescence spectrum was obtained by excitation at 360 nm.

The quantum yield was calculated according to the equation: $\Phi_{F(X)} = \Phi_{F(S)} (A_S F_X/A_X F_S) (n_X/n_S)^2$. Where A is the absorbance at the excitation wavelength, F is the area under the corrected emission curve, and n is the refractive index of the solvents used. Subscripts S and X refer to the standard and to the unknown, respectively. The fluorescence quantum yield was determined by using quinine sulfate ($\Phi_{F(S)} = 0.55$) as reference with the literature method [60, 61].

IR Spectra Measurement of NBDH/Al

To a solution of **NBDH** (10 μM) in ethanol in a flask, $Al(NO_3)_3 \cdot 9H_2O$ (30 μM) was added and stirred for 2 h. The precipitate was filtrated and dried under IR lamp to constant weight and their IR spectra were collected by KBr pallet method.

Synthesis of NBDH

To a solution of 6-Hydroxy-naphthalene-2-carboxylic acid hydrazide (202 mg, 1 mmol) in ethanol (20 mL) was added 2, 4-dihydroxy-benzaldehyde (138 mg, 1 mmol) in a flask and refluxed for 6 h. After cooling to room temperature, the precipitate was filtered and recrystallized from ethanol to get compound **NBDH** (225 mg, 70%) as yellow powder [31]. m.p. 298–299. ^{1}H NMR (Fig. S1) (600 MHz, DMSO-d_6) δ (ppm) 11.98 (s, 1H), 11.56 (s, 1H), 10.11 (s, 1H), 9.99 (s, 1H), 8.54 (s, 1H), 8.42 (s, 1H), 7.92 (d, J = 9.0 Hz, 1H), 7.88 (d, J = 8.4 Hz, 1H), 7.80 (d, J = 8.4 Hz, 1H), 7.31 (d, J = 8.4 Hz, 1H), 7.18–7.20 (m, 2H), 6.37 (d, J = 8.4 Hz, 1H), 6.33 (s, 1H). ^{13}C NMR (Fig.S2) (151 MHz, DMSO-d_6) δ (ppm) 163.01, 161.12, 157.64, 149.27, 136.82, 131.82, 131.21, 128.40, 127.42, 127.01, 126.55, 124.81, 120.08, 111.08, 109.22, 108.13, 103.13, 102.99. HRMS: m/z (TOF MS ES$^-$) (Fig. S3): Calcd. for $C_{18}H_{13}N_2O_4$: 321.0875 [**NBDH**-H^+]$^-$, found: 321.0872 (Scheme 1).

Results and Discussion

Fluorescence Studies of NBDH toward Various Metal Ions

Excellent selectivity to a certain metal ions is the most important parameters for fluorescence probes, as a consequence, the fluorescence response of probe **NBDH** toward tested ions (Ag^+, Pb^{2+}, Mg^{2+}, Ca^{2+}, Na^+, Mn^{2+}, Ba^{2+}, Hg^{2+}, Co^{2+}, Ni^{2+}, Al^{3+}, Zn^{2+}, K^+, Cd^{2+}, Fe^{3+}, Cr^{3+} and Cu^{2+}) in water solution (HEPES-NaOH buffer; pH = 7.4) was firstly examined (Fig. 1). Probe **NBDH** alone showed weak emission under neutral water solution (HEPES-NaOH buffer; pH = 7.4) and the quantum yield was 0.0047, which was attributed to the cooperation between the photoinduced electrontransfer (PET) phenomenon induced by the lone pair electron of nitrogen atom of Schiff-base (-C=N-) to the naphthalene moiety and the C=N isomerization process at the excited state [47]. Moreover, upon the addition of tested metal ions, the fluorescent spectrum of **NBDH** solution showed no change except for the Al^{3+}, which induced a significant intensity enhanced (400-fold) centered at 460 nm with a high quantum yield of 0.41, and a visible color change from colorless to bright blue under the ultraviolet lamp (365 nm) at the same time, indicating the interaction of **NBDH** with Al^{3+} and highly selectivity of **NBDH** to Al^{3+}.

In order to clarify the quantitative detection ability of **NBDH** to Al^{3+}, titration experiment between **NBDH** and Al^{3+} was conducted in HEPES-NaOH buffer solution (pH = 7.4). As shown in Fig. 2, when the gradually addition of Al^{3+} up to 1.6 equivalent to the solution of **NBDH**, the fluorescence intensity reached saturation, it also revealed that a linear

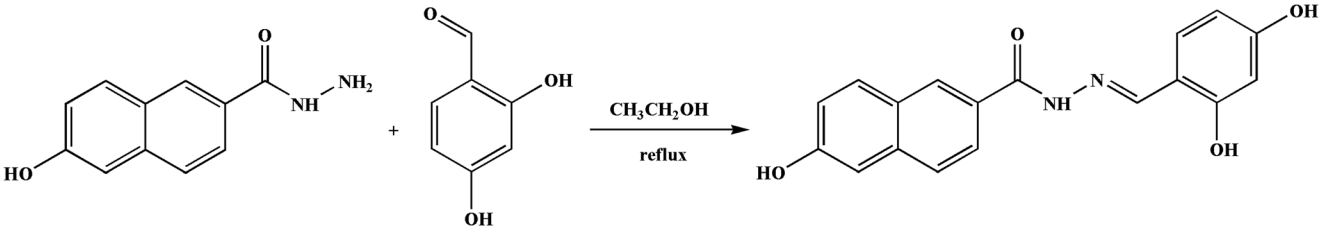

Scheme 1 Synthesis route of **NDBH**

relationship of fluorescence intensity at 460 nm with the concentration of Al^{3+} within the range of 3–20 μM (Fig. S4), and the detection limit was calculated to be 3.24 nM by applying equation 3σ/k [57].

Considering the significant fluorescence changes of probe **NBDH** towards Al^{3+}, the UV-vis absorption spectral of **NBDH** with Al^{3+} (Fig. 3) and with other different metal ions (Fig. S5) for comparison were further investigated, respectively. **NBDH** alone showed an absorbance peak at 330 nm in HEPES-NaOH buffer solution (pH = 7.4) (Fig. 3a). However, upon progressively addition of Al^{3+} (0–5 equiv.), a new peak at 320 nm emerged and increased gradually, and especially, the maximum absorbance peak of **NBDH** red shifted from 330 nm to 375 nm and its intensity increased gradually, which could be attributed the enhancement of conjugation upon the interaction of **NBDH** with Al^{3+}. More important, there was a linear relationship between data [$(A_{375}-A_{320})/A_0$] calculated by the two absorbance intensity centered at 375 nm and 320 nm (Fig. S6) and the Al^{3+} concentration ranging from 1.5 μM to 17 μM with the detection limit (LOD) calculated as 24.2 nM (Fig. S7). This result indicated that **NBDH** could be used as a ratiometric chemosensor for the detection of Al^{3+}.

Metal Ions Competition Studies

In order to further estimated the anti-interference performance of **NBDH** detection of Al^{3+} in HEPES-NaOH buffer solution (pH = 7.4), the fluorescence competition experiments of **NBDH**/Al^{3+} to other metal ions were carried out (Fig. 4). Usually, the detection of Al^{3+} was easily interfered by some metal ions, especially Fe^{3+} [47, 49], Cu^{2+} [49, 53] and Cr^{3+} [56]. However, the result showed that most metal ions actually caused negligible changes in the fluorescence intensity of **NBDH**/Al^{3+}, except for Fe^{3+}, which induced an acceptable fluorescence quenching of **NBDH**/Al^{3+} because the fluorescence signal was still strong enough for sensing Al^{3+}. Hence, this delighting result indicated that the **NBDH** was a highly selective probe for the Al^{3+} detection without disturbance of other metal ions.

Job'plot

The job'plot was conducted to confirm the binding stoichiometry between probe **NBDH** and Al^{3+}. The sum concentration of probe **NBDH** and Al^{3+} was constrained at 10 μM. The fluorescence intensity change of **NBDH**/Al^{3+} at 460 nm with the

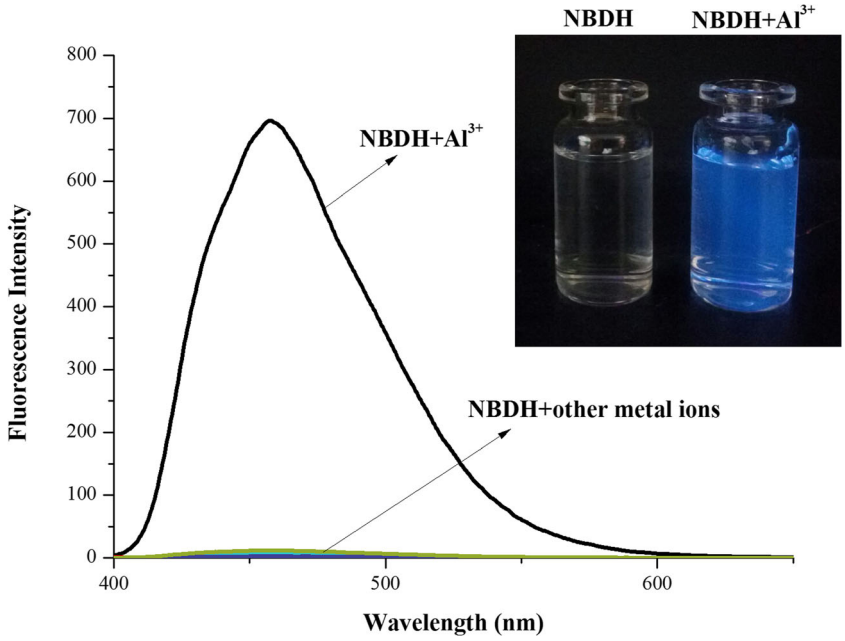

Fig. 1 Fluorescence spectral of **NBDH** (10 μM) in the presence of various metal ions (50 μM) in HEPES-NaOH buffer solution (pH = 7.4) (λ_{ex} = 360 nm). Inset: Photograph of the fluorescence change of the solution of **NBDH** (10 μM) before and after addition of Al^{3+} (50 μM) under UV light of 365 nm

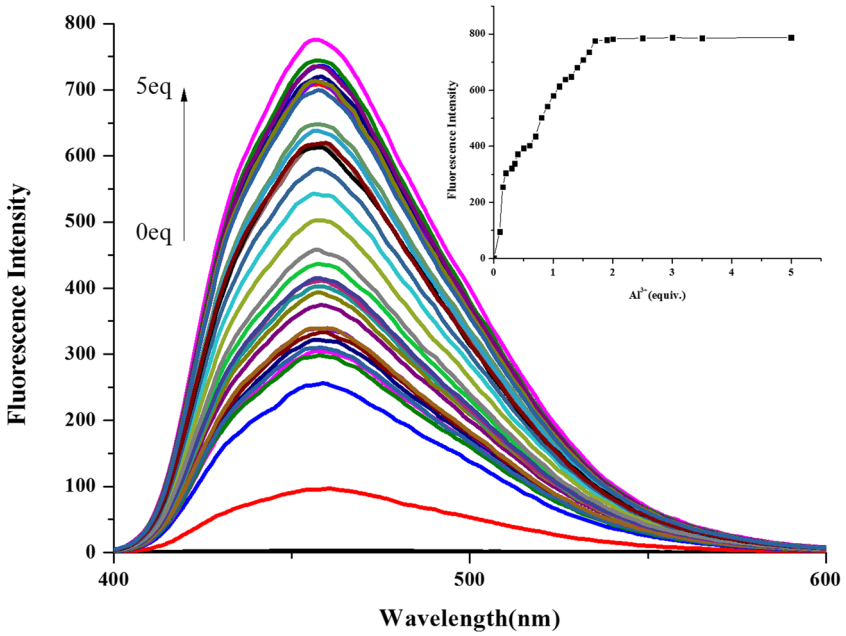

Fig. 2 Fluorescence spectra of probe **NBDH** (10 μM) towards different concentrations of Al^{3+} in HEPES-NaOH buffer solution (pH = 7.4), (λ_{ex} = 360 nm). Inset: Fluorescence intensity at 460 nm versus the number of equiv. of Al^{3+} added, (λ_{ex} = 360 nm)

mole fraction of Al^{3+} within the range of 0 to 0.9 was measured (Fig. 5). Maximum fluorescence intensity at 460 nm reached at 0.5 of mole fraction ([Al^{3+}]/[**NBDH** + Al^{3+}]), indicating a 1:1 binding mode for **NBDH**/Al^{3+} complex. Moreover, according to the Benesi-Hildebrand plot [56, 57], the association constant of probe **NBDH** for Al^{3+} was confirmed to be 6.30×10^4 M^{-1} (Fig. S8) and 1.82×10^4 M^{-1} (Fig. S9), which were calculated based on the fluorescence titration data and the absorbance titration data, respectively.

Effect of pH and Time

In order to estimate whether probe **NBDH** has a good performance for sensing Al^{3+} in water solution, the pH effect on the fluorescence response of probe **NBDH** toward Al^{3+} with the pH range from 2.0 to 12.0 was investigated (Fig. S10). It showed that there was nearly no fluorescence emission of free probe **NBDH** solution under the condition of in the pH <4.0 or pH >7.0. However, probe **NBDH** solution exhibited a prominent response in the presence of Al^{3+} in the range of pH = 7–8. The result indicated that probe **NBDH** could be used an ideal Al^{3+} probe in physiological condition.

In addition, the time-dependent response assay was carried out to investigate the fluorescence and absorbance of **NBDH** with the addition of Al^{3+}. The result showed that a stable response of **NBDH** with Al^{3+} was obtained at maximum within less 5 min (Fig. S11). Once a plateau was attained, both the intensity of fluorescence and absorbance were maintained

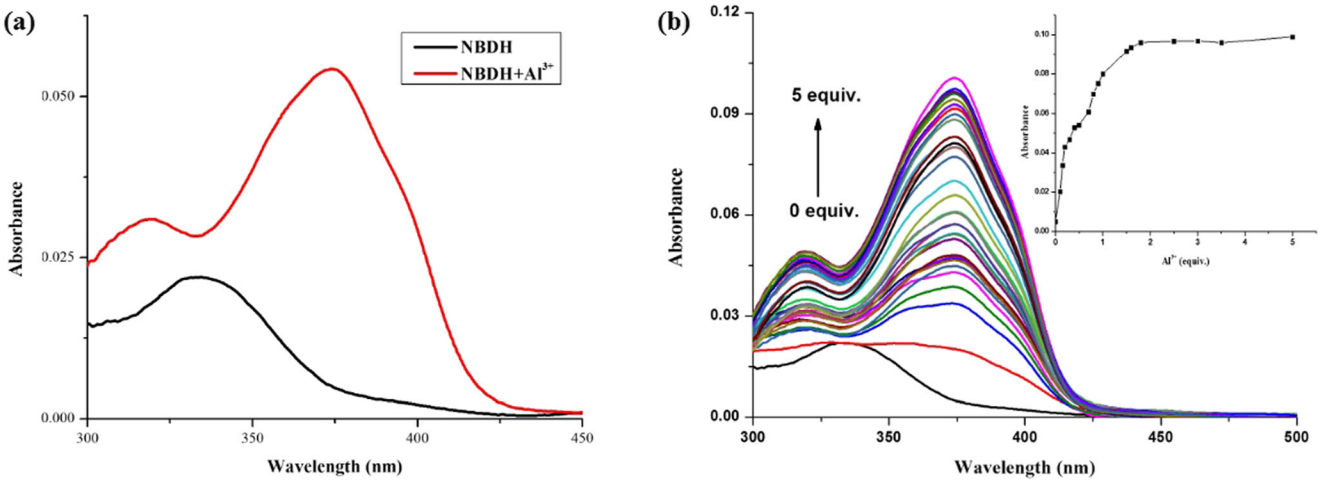

Fig. 3 **a** UV-vis absorption spectral change of **NBDH** (10 μM) in presence of five equivalent amount of Al^{3+} in HEPES-NaOH buffer solution (pH = 7.4); **b** UV-vis absorption of probe **NBDH** (10 μM) towards different concentrations of Al^{3+} in HEPES-NaOH buffer solution (pH = 7.4). Inset: Absorbance intensity at 375 nm versus the number of equiv. of Al^{3+} added

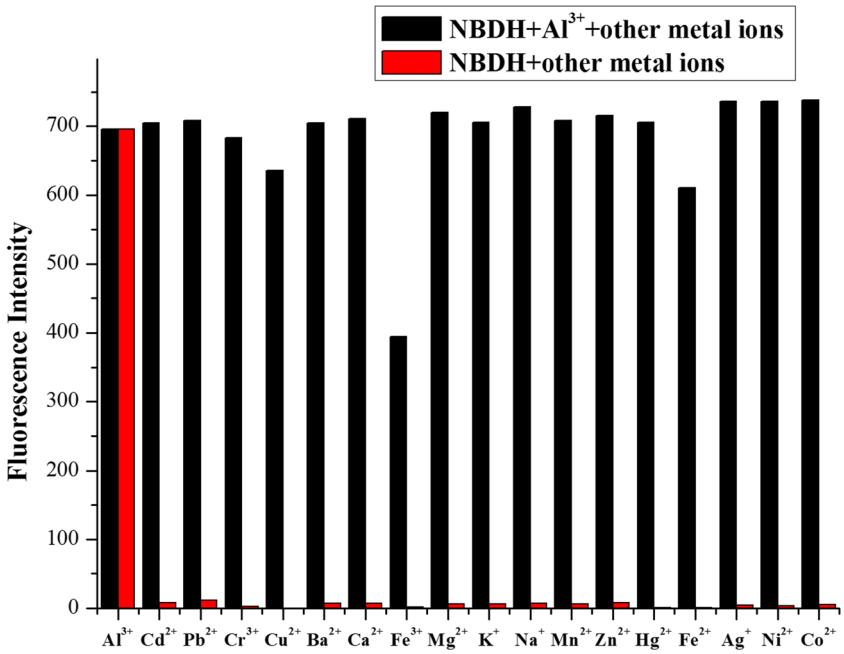

Fig. 4 Fluorescence intensity at 460 nm of **NBDH** (10 μM) upon addition of various metal ions (50 μM) in the presence Al^{3+} (50 μM) in HEPES-NaOH buffer solution (pH = 7.4), (λ_{ex} = 360 nm)

relatively stable for the measurement, indicating that **NBDH** exhibits good photostability.

Study on Response Mechanism

Mass Spectrometry Analysis

To further confirm the formation of coordinated complex between the probe **NBDH** and Al^{3+}, the mass spectrometry analysis that **NBDH** (10 mM) in presence 3 equiv. Al^{3+} in the solution of ethanol solution were carried out. The HRMS spectrum exhibited peaks at m/z 411.1122, m/z 425.1280 and m/z 439.1074 were corresponded to [**NBDH**-$2H^+$+Al^{3+}+$C_2H_5OH + H_2O$]$^+$ (calcd. m/z: 411.1137), [**NBDH**-$2H^+$+Al^{3+}+$C_2H_5OH + CH_3OH$]$^+$ (calcd. m/z: 425.1293) and [**NBDH**-$2H^+$+Al^{3+}+$2C_2H_5OH$]$^+$ (calcd. m/z: 439.1450) (Fig. 6), respectively.

FT-IR Spectral and ^{1}H NMR Titration Experiments

The evidence for the **NBDH**/Al^{3+} coordination was obtained from FT-IR spectral data exhibited in Fig. S12. Compared

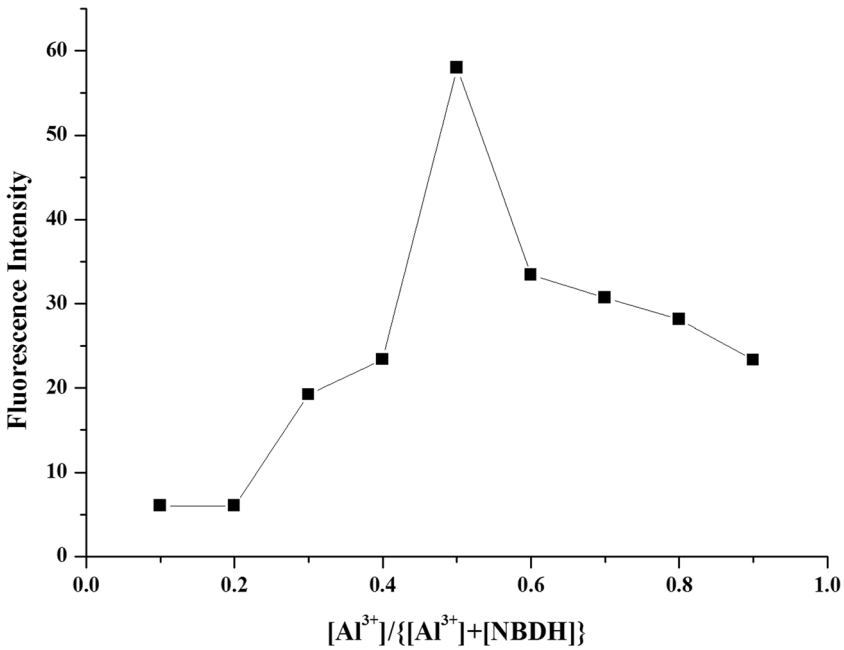

Fig. 5 Job's plot of the complexation between **NBDH**/Al^{3+}

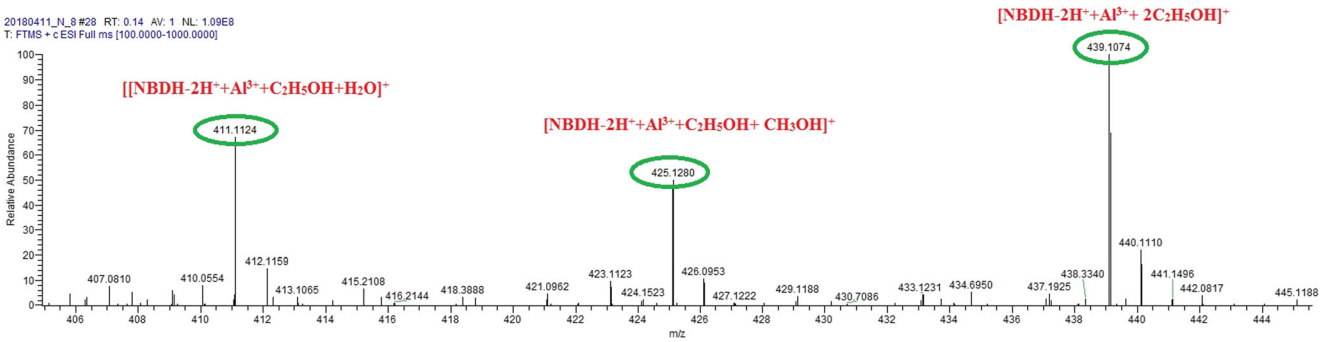

Fig. 6 ESI-MS spectra of **NBDH**/Al^{3+} in ethanol

with the IR spectra of **NBDH** itself, the peak at 3180 cm^{-1} (O-H) shifted to 3090 cm^{-1} (O-H), peak at 1618 cm^{-1} (C=O) changed into weak absorbance and shifted to 1623 cm^{-1}, and peak at 1496 cm^{-1} (C=N) remarkably shifted to 1348 cm^{-1} in the FT-IR spectra of **NBDH**/Al^{3+}. Moreover, the bands at about 795 and cm^{-1} 598 cm^{-1} were assigned to (Al-O)[[46] and (Al-N),[[53] respectively. The above results indicated that the O atom and N atom of enolization of amide group (-CONH-) and the two imide N atoms may be involved in the coordination of **NBDH** with Al^{3+}. In order to make clear binding sites of **NBDH** with Al^{3+}, ^{1}H NMR titration experiments were carried out, and the results were depicted in Fig. 7. Upon the addition of Al^{3+}, the proton signals of amide group (H_b) and hydroxy group (H_d) were all disappeared, indicated the occurrence of deprotonation during the process of coordination with Al^{3+}, which further supported the result concluded by FT-IR spectral.

According to the above results, the proposed sensing mechanism of **NBDH** to Al^{3+} was illustrated in scheme 2. Moreover, comparison of **NBDH** with some reported Al^{3+}

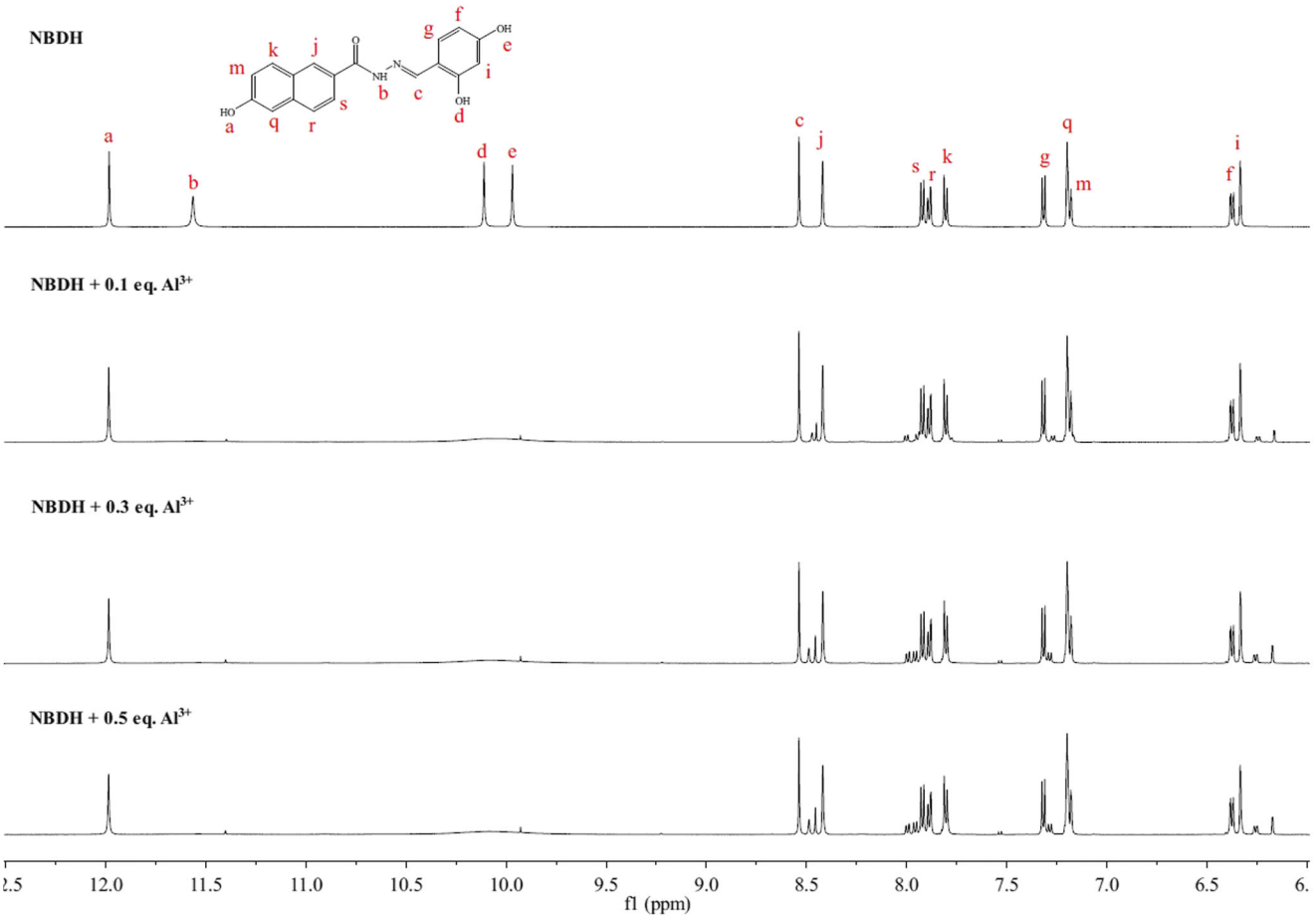

Fig. 7 ^{1}H NMR spectra of **NBDH** with Al^{3+} in DMSO d_6

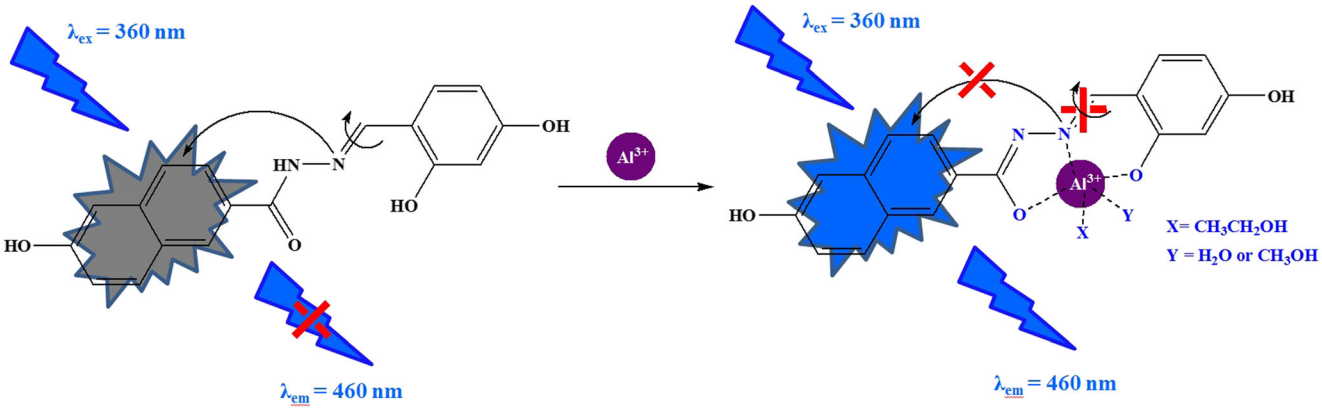

Scheme 2 Proposed sensing mechanism of **NBDH** for Al^{3+}

fluorescent probes was summarized in Table 1. Compared with the similar naphthalene Schiff's base sensor [25, 39–42, 59], the interesting factors of **NBDH** was its absolute solubility in water and lower detection limit.

Applications

Detection of Al^{3+} in Real Water Samples

In order to estimate the practicability of **NBDH**, the amount of Al^{3+} in real water samples obtained from our campus was detected, and the results were listed in Table 2. The data showed a good agreement between the added and the found concentration of Al^{3+}. Moreover, real environmental aqua objects in Songhua River were further detected, and the results showed that a linear relationship of fluorescence intensity at 460 nm with the concentration of Al^{3+} within the range of 10–50 μM (Fig. S13-S14). Therefore, the above results indicated that **NBDH** can be competent for Al^{3+} detection in environmental analysis.

Detection of Al^{3+} on Test Paper

In order to development of portable and convenient method to detection of Al^{3+}, the test paper experiment was conducted. The test paper was immersed in different concentration

Table 1 Comparison of different properties of **NBDH** with recently reported fluorescent probes for Al^{3+}

Ref.	Methods of detection	Detection Medium	LOD	Binding Constants	Mechanism	pH range	Application
[25]	Fluorescent (turn on)	CH_3OH/H_2O (7:3)	1.0×10^{-7} M	1.83×10^5 $M^{-1/2}$	ICT, CHEF and C=N isomerization	6–8	Cell imaging
[39]	Fluorescent (turn on)	H_2O	4.3×10^{-6} M	5.17×10^4 M^{-1}	PET and ESIPT	NR	NR
[40]	Fluorescent (turn on)	DMF/H_2O (99:1)	4×10^{-6} M	4×10^3 M^{-1}	PET and ESIPT	NR	NR
[42]	Fluorescent (turn on)	C_2H_5OH/H_2O (1:1)	3.7×10^{-7} M	7.62×10^6 M^{-1}	CHEF	NR	Cell imaging
[43]	Fluorescent (turn on)	C_2H_5OH/H_2O (95:5)	1.08×10^{-7} M	6.53×10^3 M^{-1}	PET	2–7	Cell imaging
[52]	Fluorescent (turn on)	CH_3OH/H_2O (9:1)	1.62×10^{-6} M	9.9×10^3 M^{-1}	CHEF	6.5–10	Cell imaging
[53]	Fluorescent (turn on)	C_2H_5OH/H_2O (3:1)	3.48×10^{-8} M	1.30×10^4 M^{-1}	PET and C=N isomerization	4–11	Cell imaging Soild state probe
[54]	Fluorescent (turn on)	DMF/H_2O (4:1)	3.9×10^{-7} M	8.5×10^5 M^{-1}	AIE	NR	Real sample
[55]	Fluorescent (turn on)	CH_3OH/H_2O (9:1)	1.34×10^{-6} M	1.06×10^4 M^{-1}	CHEF	7–11	Cell imaging
[56]	Fluorescent (turn on)	CH_3CN	3.1×10^{-7} M	5.44×10^4 M^{-1}	ESIPT and C=N isomerization	8.5	NR
[57]	Fluorescent (turn on)	CH_3OH	8.08×10^{-8} M	1.57×10^5 M^{-1}	ICT and ESIPT	NR	Cell imaging
[59]	Fluorescent (turn on)	DMF/H2O (1: 9)	1.92×10^{-7} M	6.6×10^4 M^{-1}	ESIPT and CHEF	4–8	Cell imaging
This work	Ratiometric absorbance Fluorescent (turn on)	H_2O	2.42×10^{-8} M	1.57×10^4 M^{-1}	PET and C=N isomerization	7–8	Real sample
			3.24×10^{-9} M	6.30×10^4 M^{-1}			Test paper

LOD The limit of detection, *NR* Not reported in the corresponding paper

Table 2 Determination of Al^{3+} in water samples from different water sources

Water samples	Amount of standard Al^{3+} added (μmol/L)	Total Al^{3+} found ($n = 3$) (μmol/L)	Recovery of Al^{3+} (n = 3) added (%)	RSD (%)	Relative error (%)
ultrapure water	14	14.29	102.07	1.57	2.42
	15	15.54	103.60	1.36	3.86
	16	15.89	99.31	2.08	−0.69
Tap water (Department of Chemistry)	14	14.50	103.57	2.52	4.17
	15	15.62	104.13	1.53	4.43
	16	16.40	102.50	0.91	2.50

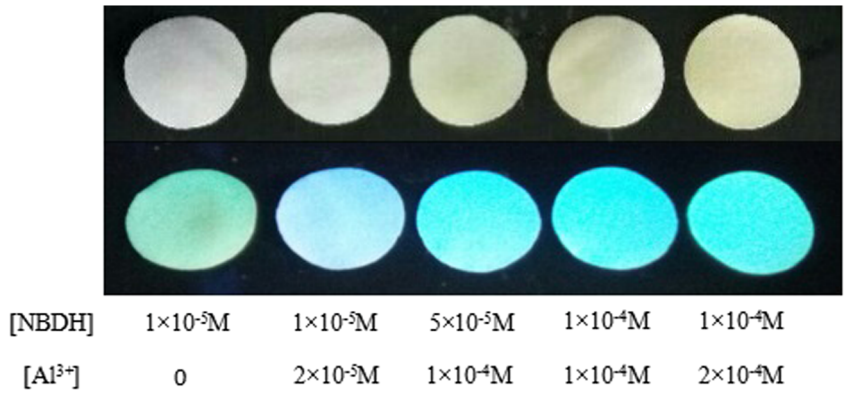

Fig. 8 Color changes of filter paper after immersing in EtOH solution of different concentration **NBDH** (100 μM) containing different equiv. Al^{3+} (0–400 μM). Top: under natural light, bottom: under a ZF-1A ultraviolet analyzer (Shanghai Qinke Instrument Equipment Co., Ltd.)

NBDH (10^{-5} M, 5×10^{-5} M and 10^{-4} M) ethanol solution containing different Al^{3+} (1–2 equiv.) and then dried in air. As shown in Fig. 8, both the visual color change (from colorless to yellow) and fluorescence color change (from green to blue) under ultraviolet lamp (365 nm) were clearly observed. Hence, this test paper, detection Al^{3+} using colorimetric method by naked eye, has potential application in environmental monitoring.

Conclusions

In conclusion, an excellent naphthalene-based probe **NBDH** was designed and synthesized. It can be achieved in fluorescent "turn-on" and ratiometric detection of Al^{3+} in HEPES/NaOH buffer (pH = 7.4) based on coordinated effects of PET and the inhibition of C=N isomerization. The coordination mode of **NBDH**/Al^{3+} was confirmed 1:1 by job' plot, FT-IR, ^{1}H NMR and HRMS. Furthermore, **NBDH** was successfully applied in test paper for the colorimetric detection Al^{3+}.

Acknowledgements This work was supported by by the Research Science Foundation in Technology Innovation of Harbin (No. 2017RAQXJ022) and Postdoctoral Scientific Research Developmental Fund of Heilongjiang Province (No. LBH-Q14023).

References

1. Liu YJ, Tian FF, Fang XY, Jiang FL, Liu Y (2017) Fabrication of an acylhydrazone based fluorescence probe for Al^{3+}. Sensors Actuators B Chem 240:916–925. https://doi.org/10.1016/j.snb.2016.09.051
2. Sasitharan K, Varghese A, George L (2017) Flavonol based surface modification of doped chalcogenide nanoflakes as an ultrasensitive fluorescence probe for Al^{3+} ion. Anal Chim Acta 992:94–104. https://doi.org/10.1016/j.aca.2017.08.045
3. Wen XY, Fan ZF (2016) Linear Schiff-base fluorescence probe with aggregation-induced emission characteristics for Al^{3+} detection and its application in live cell imaging. Anal Chim Acta 945:75–84. https://doi.org/10.1016/j.aca.2016.09.036
4. Zhang XX, Wang RJ, Liu G, Fan CB, Pu SZ (2016) A highly selective fluorescence probe for Al^{3+} based on a new diarylethene with a 6-(hydroxymethyl)picolinohydrazide unit. Tetrahedron 72:8449–8455. https://doi.org/10.1016/j.tet.2016.11.007
5. Dhineshkumar E, Iyappan M, Anbuselvan C (2018) Turn on macrocyclic chemosensor for Al^{3+} ion with facile synthesis and application in live cell imaging. Spectrochim Acta A Mol Biomol Spectrosc 199:209–219. https://doi.org/10.1016/j.saa.2018.03.053
6. Zhu Q, Li L, Mu L, Zeng X, Redshaw C, Wei G (2016) A ratiometric Al^{3+} ion probe based on the coumarin-quinoline FRET system. J Photochem Photobiol A 328:217–224. https://doi.org/10.1016/j.jphotochem.2016.06.006
7. Wang Y, Ma ZY, Zhang DL, Deng JL, Chen X, Xie CZ, Qiao X, Li QZ (2018) Xu JY, highly selective and sensitive turn-on fluorescent sensor for detection of Al^{3+} based on quinoline-base Schiff base. Spectrochim Acta A Mol Biomol Spectrosc 195:157–164. https://doi.org/10.1016/j.saa.2018.01.049

8. Pang BJ, Li CR, Yang ZY (2018) Design of a colorimetric and turn-on fluorescent probe for the detection of Al (III). J Photochem Photobiol A 356:159–165. https://doi.org/10.1016/j.jphotochem.2017.12046
9. Wu WN, Mao PD, Wang Y, Zhao XL, Jia L, Xu ZY (2016) Rhodamine 6G hydrazone bearing thiophene unit: a highly sensitive and selective offeon fluorescent chemosensor for Al^{3+}. J Mol Struct 1122:24–28. https://doi.org/10.1016/j.molstruc.2016.05.074
10. Kumara M, Kumara A, Faizi MSH, Kumara S, Singh MK, Sahu SK, Kishor S, John RP (2018) A selective "turn-on" fluorescent chemosensor for detection of Al^{3+} in aqueous medium: experimental and theoretical studies. Sensors Actuators B Chem 260:888–899. https://doi.org/10.1016/j.snb.2018.01.098
11. Li DP, Han XJ, Yan ZQ, Cui Y, Miao JY, Zhao BX (2018) A far-red ratiometric fluorescent probe for SO_2 derivatives based on the ESIPT enhanced FRET platform with improved performance. Dyes Pigments 151:95–101. https://doi.org/10.1016/j.dyepig.2017.12.056
12. Kang L, Xing ZY, Ma XY, Liu YT, Zhang Y (2016) A highly selective colorimetric and fluorescent turn-on chemosensor for Al^{3+} based on naphthalimide derivative. Spectrochim Acta A Mol Biomol Spectrosc 167:59–65. https://doi.org/10.1016/j.saa.2016.05.030
13. Li NN, Ma YQ, Zeng S, Liu YT, Sun XJ, Xing ZY (2017) A highly selective colorimetric and fluorescent turn-on chemosensor for Zn^{2+} and its logic gate behavior. Synth Met 232:17–24. https://doi.org/10.1016/j.synthmet.2017.07.017
14. Naskar B, Modak R, Sikdar Y, Maiti DK, Bauzá A, Frontera A, Katarkar A, Chaudhuri K, Goswami S (2017) Fluorescent sensing of Al^{3+} by benzophenone based Schiff base chemosensor and live cell imaging applications: impact of keto-enol tautomerism. Sensors Actuators B Chem 239:1194–1204. https://doi.org/10.1016/j.snb.2016.08.148
15. Kang L, Liu YT, Li NN, Dang XX, Xing ZY, Li JL, Zhang Y (2017) A schiff-base receptor based naphthalimide derivative: highly selective and colorimetric fluorescent turn-on sensor for Al^{3+}. J Lumin 186:48–52. https://doi.org/10.1016/j.jlumin.2016.12.056
16. Zhang XX, Wang RJ, Liu G, Fang CB, Pu SZ (2016) A highly selective fluorescence probe for Al^{3+} based on a new diarylethene with a 6-(hydroxymethyl)picolinohydrazide unit. Tetrahedron 72:8449–8455. https://doi.org/10.1016/j.tet.2016.11.007
17. Li NN, Zeng S, Li MQ, Ma YQ, Sun XJ, Xing ZY, Li JL (2018) A highly selective naphthalimide-based chemosensor: "naked-eye" colorimetric and fluorescent turn-on recognition of Al^{3+} and its application in practical samples, test paper and logic gate. J Fluoresc 28:347–357. https://doi.org/10.1007/s10895-017-2197-9
18. Maniyazagana M, Mariadasseb R, Nachiappanb M, Jeyakanthanb J, Lokanath NK, Naveenc S, Sivaramand G, Muthurajaa P, Manisankar P, Stalina T (2018) Synthesis of rhodamine based organic nanorods for efficient chemosensor probe for Al (III) ions and its biological applications. Sensors Actuators B Chem 254:795–804. https://doi.org/10.1016/j.snb.2017.07.106
19. Zhou YM, Zhang JL, Zhou H, Hu XY, Zhang L, Zhang M (2013) A highly selective fluorescent probe for Al^{3+} based on 4-aminoantipyrine. Spectrochim Acta A Mol Biomol Spectrosc 106:68–72. https://doi.org/10.1016/j.saa.2012.12.084
20. Sen B, Sheet SK, Thounaojam R, Jamatia R, Pal AK, Aguan K, Khatua S (2017) A coumarin based Schiff base probe for selective fluorescence detection of Al^{3+} and its application in live cell imaging. Spectrochim Acta A Mol Biomol Spectrosc 173:537–543. https://doi.org/10.1016/j.saa.2016.10.005
21. Diao QP, Ma PY, Lv LL, Li TC, Sun Y, Wang XH, Song DQ (2016) A water-soluble and reversible fluorescent probe for Al^{3+} and F^- in living cells. Sensors Actuators B Chem 229:138–144. https://doi.org/10.1016/j.snb.2016.01.136
22. Janakipriya S, Chereddy NR, Korrapati P, Thennarasu S, Mandal AB (2016) Selective interactions of trivalent cations Fe^{3+}, Al^{3+} and Cr^{3+} turn on fluorescence in a naphthalimide based single molecular probe. Spectrochim Acta A Mol Biomol Spectrosc 153:465–470. https://doi.org/10.1016/j.saa.2015.08.044
23. Yue XL, Li CR, Yang ZY (2017) A novel Schiff-base fluorescent probe based on 1,8-naphthyridine and naphthalimide for Al^{3+}. Inorg Chim Acta 464:167–171. https://doi.org/10.1016/j.ica.2017.05.032
24. Gupta A, Kumar N (2016) A review of mechanisms for fluorescent "turn-on" probes to detect Al^{3+} ions. RSC Adv 6:106413–106434. https://doi.org/10.1039/c6ra23682k
25. Wang RJ, Wang NS, Pu SZ, Zhang XX, Liu G, Dai YF (2017) A acid/base gated photochromic and fluorescent sensor based on a diarylethene with a 2-(1H-dithienobenzoimidazole)phenol unit. Dyes Pigments 146:445–454. https://doi.org/10.1016/j.dyepig.2017.07.036
26. Liu HY, Zhang BB, Tan CY, Liu F, Cao JK, Tan Y, Jiang YY (2016) Simultaneous bioimaging recognition of Al^{3+} and Cu^{2+} in living-cell, and further detection of F^- and S^{2-} by a simple fluorogenic benzimidazole-based chemosensor. Talanta 161:309–319. https://doi.org/10.1016/j.talanta.2016.08.061
27. Feng ET, Lu RM, Fan CB, Zheng CH, Pu SZ (2017) A fluorescent sensor for Al^{3+} based on a photochromic diarylethene with a hydrazinobenzothiazole Schiff base unit. Tetrahedron Lett 58:1390–1394. https://doi.org/10.1016/j.tetlet.2017.02.067
28. Maniyazagan M, Mariadasse R, Nachiappan M, Jeyakanthan J, Lokanathc NK, Naveen S, Sivaraman G, Muthuraja P, Manisankar P, Stalin T (2018) Synthesis of rhodamine based organic nanorods for efficientchemosensor probe for Al (III) ions and its biological applications. Sensors Actuators B Chem 254:795–804. https://doi.org/10.1016/j.snb.2017.07.106
29. Singh R, Samanta S, Mullick P, Ramesh A, Das G (2018) Al^{3+} sensing through different turn-on emission signals Vis-a-Vis two different excitations: applications in biological and environmental realms. Anal Chim Acta 1025:172–180. https://doi.org/10.1016/j.aca.2018.03.053
30. Sarkar D, Ghosh P, Gharami S, Mondal TK, Murmu N (2017) A novel coumarin based molecular switch for the sequential detectionof Al^{3+} and F^-: application in lung cancer live cell imaging andconstruction of logic gate. Sensors Actuators B Chem 242:338–346. https://doi.org/10.1016/j.snb.2016.11.059
31. Liao Z, Liu Y, Han SF, Wang D, Zheng JQ, Zheng XJ, Jin LP (2017) A novel acylhydrazone-based derivative as dual-mode chemosensorfor Al^{3+}, Zn^{2+} and Fe^{3+} and its applications in cell imaging. Sensors Actuators B Chem 244:914–921. https://doi.org/10.1016/j.snb.2017.01.074
32. Yao DH, Huang XW, Guo FQ, Xie PH (2018) A new fluorescent enhancement chemosensor for Al^{3+} and Fe^{3+} based on naphthyridine and benzothiazole groups. Sensors Actuators B Chem 256:276–281. https://doi.org/10.1016/j.snb.2017.10.080
33. Rai A, Singh AK, Tripathi K, Sonkar AK, Chauhan BS, Srikrishna S, James TD, Mishra L (2018) A quick and selective rhodamine based "smart probe" for "signal-on"optical detection of Cu^{2+} and Al^{3+} in water, cell imaging, computational studies and solid state analysis. Sensors Actuators B Chem 266:95–105. https://doi.org/10.1016/j.snb.2018.02.019
34. Sen B, Sheet SK, Thounaojam R, Jamatia R, Pal AK, Aguan K, Khatua S (2017) A coumarin based Schiff base probe for selective fluorescence detection of Al^{3+} and its application in live cell imaging. Spectrochim Acta A Mol Biomol Spectrosc 173:537–543. https://doi.org/10.1016/j.saa.2016.10.005
35. Yue XL, Wang ZQ, Li CR, Yang ZY (2018) A highly selective and sensitive fluorescent chemosensor and its application for rapid on-site detection of Al^{3+}. Spectrochim Acta A Mol Biomol Spectrosc 193:415–421. https://doi.org/10.1016/j.saa.2017.12.053

36. Xu JC, Zhang Y, Zeng LT, Liu JB, Kinsella JM, Sheng RL (2016) A simple naphthalene-based fluorescent probe for high selective detection of formaldehyde in toffees and HeLa cells via aza-cope reaction. Talanta 160:645–652. https://doi.org/10.1016/j.talanta.2016.08.010
37. Santhoshkumar S, Velmurugan K, Prabhu J, Radhakrishnan G, Nandhakumar R (2016) A naphthalene derived Schiff base as a selective fluorescent probe for Fe^{2+}. Inorg Chim Acta 439:1–7. https://doi.org/10.1016/j.ica.2015.09.030
38. Sahana A, Banerjee A, Lohar S, Das S, Hauli I, Mukhopadhyay SK, Matalobos JS, Das D (2013) Naphthalene based highly selective OFF-ON-OFF type fluorescent probe for Al^{3+} and NO_2 ions for living cell imaging at physiological pH. Inorg Chim Acta 398:64–71. https://doi.org/10.1016/j.ica.2012.12.012
39. Yue XL, Wang ZQ, Li CR, Yang ZY (2017) Naphthalene-derived Al^{3+}-selective fluorescent chemosensor based on PET and ESIPT in aqueous solution. Tetrahedron Lett 58:4532–4537. https://doi.org/10.1016/j.tetlet.2017.10.044
40. Qin JC, Yang ZY, Yang P (2015) Recognition of Al^{3+} based on a naphthalene-based "off–on" chemosensor in near 100% aqueous media. Inorg Chim Acta 432:136–141. https://doi.org/10.1016/j.ica.2015.03.029
41. Roy A, Dey S, Halder S, Roy P (2017) Development of a new chemosensor for Al^{3+} ion: tuning of properties. J Lumin 192:504–512. https://doi.org/10.1016/j.jlumin.2017.07.020
42. Wang QM, Sun HF, Jin L, Wang WL, Zhang ZH, Chen YL (2018) A novel turn on and reversible sensor for Al^{3+} and its applications in bioimaging. J Lumin 203:113–120. https://doi.org/10.1016/j.jlumin.2018.06.047
43. Zhu JL, Zhang YH, Wang L, Sun TM, Wang M, Wang YP, Ma DY, Yang QQ, Tang YF (2016) A simple turn-on Schiff base fluorescence sensor for aluminum ion. Tetrahedron Lett 57:3535–3539. https://doi.org/10.1016/j.tetlet.2016.06.112
44. Das B, Dey S, Maiti GP, Bhattacharjee A, Dhara A, Jana A (2018) Hydrazinopyrimidine derived novel Al^{3+} chemosensor: molecular logic gate and biological applications. New J Chem 42:9424–9435. https://doi.org/10.1039/c7nj05095j
45. Jo TG, Jung JM, Han J, Lim MH, Kim C (2017) A single fluorescent chemosensor for multiple targets of Cu^{2+}, $Fe^{2+/3+}$ and Al^{3+} in living cells and a near-perfect aqueous solution. RSC Adv 7:28723–28732. https://doi.org/10.1039/c7ra05565j
46. Wen XY, Fan ZF (2016) Linear Schiff-base fluorescence probe with aggregation-induced emission characteristics for Al^{3+} detection and its application in live cell imaging. Anal Chim Acta 945:75–84. https://doi.org/10.1016/j.aca.2016.09.036
47. Li CR, Li SL, Yang ZY (2016) A chromone-derived Schiff-base as Al^{3+} "turn-on" fluorescent probe based on photoinduced electron-transfer (PET) and C=N isomerization. Tetrahedron Lett 57:4898–4904. https://doi.org/10.1016/j.tetlet.2016.09.058
48. Yue XL, Li CR, Yang ZY (2017) A novel Schiff-base fluorescent probe based on 1,8-naphthyridine and naphthalimide for Al^{3+}. Inorg Chim Acta 464:167–171. https://doi.org/10.1016/j.ica.2017.05.032
49. Hossain SM, Singh K, Lakma A, Pradhan RN, Singh AK (2017) A schiff base ligand of coumarin derivative as an ICT-based fluorescence chemosensor for Al^{3+}. Sensors Actuators B Chem 239:1109–1117. https://doi.org/10.1016/j.snb.2016.08.093
50. Naskar B, Modak R, Sikdar Y, Maiti DK, Bauzá A, Frontera A, Katarkar A, Chaudhuri K, Goswami S (2017) Fluorescent sensing of Al^{3+} by benzophenone based Schiff base chemosensor and live cell imaging applications: impact of keto-enol tautomerism. Sensors Actuators B Chem 239:1194–1204. https://doi.org/10.1016/j.snb.2016.08.148
51. Li W, Tian XH, Huang B, Li HJ, Zhao XY, Gao S, Zheng J, Zhang XZ, Zhou HP, Tian YP, Wu JY (2016) Triphenylamine-based Schiff bases as the high sensitive Al^{3+} or Zn^{2+} fluorescence turn-on probe: mechanism and application *in vitro* and *in vivo*. Biosens Bioelectron 77:530–536. https://doi.org/10.1016/j.bios.2015.09.059
52. Sheet SK, Sen B, Thounaojam R, Aguan K, Khatua S (2017) Highly selective light-up Al^{3+} sensing by a coumarin based Schiff base probe: subsequent phosphate sensing DNA binding and live cell imaging. J Photochem Photobiol A 332:101–111. https://doi.org/10.1016/j.jphotochem.2016.08.019
53. Pang BJ, Li CR, Yang ZY (2018) Design of a colorimetric and turn-on fluorescent probe for the detection of Al (III). J Photochem Photobiol A 356:159–165. https://doi.org/10.1016/j.jphotochem.2017.12.046
54. Wang Q, Wen XY, Fan ZF (2018) A Schiff base fluorescent chemsensor for the double detection of Al^{3+} and PPi through aggregation induced emission in environmental physiology. J Photochem Photobiol A 358:92–99. https://doi.org/10.1016/j.jphotochem.2018.03.004
55. Sen B, Sheet SK, Thounaojam R, Jamatia R, Pal AK, Aguan K, Khatua S (2017) A coumarin based Schiff base probe for selective fluorescence detection of Al^{3+} and its application in live cell imaging. Spectrochim Acta A Mol Biomol Spectrosc 173:537–543. https://doi.org/10.1016/j.saa.2016.10.005
56. Tajbakhsh M, Chalmardi GB, Bekhradnia A, Hosseinzadeh R, Hasani N, Amiri MA (2018) A newfluorene-based Schiff-base as fluorescent chemosensor for selective detection of Cr^{3+} and Al^{3+}. Spectrochim Acta A Mol Biomol Spectrosc 189:22–31. https://doi.org/10.1016/j.saa.2017.08.007
57. Wang Y, Ma ZY, Zhang DL, Deng JL, Chen X, Xie CZ, Qiao X, Li QZ, Xu JY (2018) Highly selective and sensitive turn-on fluorescent sensor for detection of Al^{3+} based on quinoline-base Schiff base. Spectrochim Acta A Mol Biomol Spectrosc A 195:157–164. https://doi.org/10.1016/j.saa.2018.01.049
58. Qin JC, Cheng XY, Fang R, Wang MF, Yang ZY, Li TR, Li Y (2016) Two Schiff-base fluorescent sensors for selective sensing of aluminum (III): experimental and computational studies. Spectrochim Acta A Mol Biomol Spectrosc A 152:352–357. https://doi.org/10.1016/j.saa.2015.07.095
59. Zeng S, Li SJ, Sun XJ, Li MQ, Ma YQ, Xing ZY, Li JL (2018) A naphthalene-quinoline based chemosensor for fluorescent "turn-on" and absorbance-ratiometric detection of Al3+ and its application in cells imaging. Spectrochim Acta A Mol Biomol Spectrosc A 205:276–286. https://doi.org/10.1016/j.saa.2015.07.095
60. Tong L, Qian Y (2019) A naphthalimide–rhodamine chemodosimeter for hypochlorite based on TBET: high quantum yield and endogeous imaging in living cells. J Photochem Photobiol A 368:62–69. https://doi.org/10.1016/j.jphotochem.2018.09.027
61. Olmsted J (1979) Calorimetric determinations of absolute fluorescence quantum yields. J Phys Chem 83:2581–2584. https://doi.org/10.1021/j100483a006